ACS APPLIED ELECTRONIC MATERIALS

pubs.acs.org/acsaelm

Article

Sustainable Multi-stack Printed Heaters on Paper with Efficient Heat Distribution

Published as part of ACS Applied Electronic Materials special issue "Sustainable Development of Printed Electronics: From Materials Processing to Devices Implementation".

Dorina T. Papanastasiou,* Daniel Morais, Raquel Azevedo Martins, Elvira Fortunato, Rodrigo Martins, Pedro Barquinha, and Emanuel Carlos*

Cite This: ACS Appl. Electron. Mater. 2025, 7, 4862−4871

Read Online

ACCESS | Metrics & More | Article Recommendations | Supporting Information

ABSTRACT: Printed heaters are emerging as a promising solution for flexible, sustainable, and eco-friendly applications, with potential uses ranging from wearable and portable devices to the automotive industry. This study addresses key challenges in heat uniformity and mechanical protection, by employing screen printing with water-based inks and biodegradable paper substrates. The multi-stack heater, composed of carbon, silver, and aluminum oxide ($C/Ag/AlO_x$), demonstrates excellent electrical and thermal performance. At 5 V, the $C/Ag/AlO_x$ heater achieves a peak temperature of approximately 120 °C, with spatial temperature fluctuations within ±3 °C, offering superior thermal uniformity compared to bare Ag and Ag/AlO_x heaters, which exhibit temperature gradients up to 10 °C. All configurations show robust durability during 6 h of 5 V cycling and minimal resistance changes during environmental stability tests under 80 °C and 80% relative humidity. In tape adhesion tests, the $C/Ag/AlO_x$ heater maintained nearly unchanged resistance after several peel cycles thanks to the protective AlO_x coating. Finally, the ultralow cost multi-stack configuration (0.20 € per heater) embedded in a skin bandage reached a maximum temperature of 50 °C at 3.5 V, with a power density of 0.08 W/cm^2, highlighting its potential for precise temperature control and homogeneous heating in thermotherapy applications.

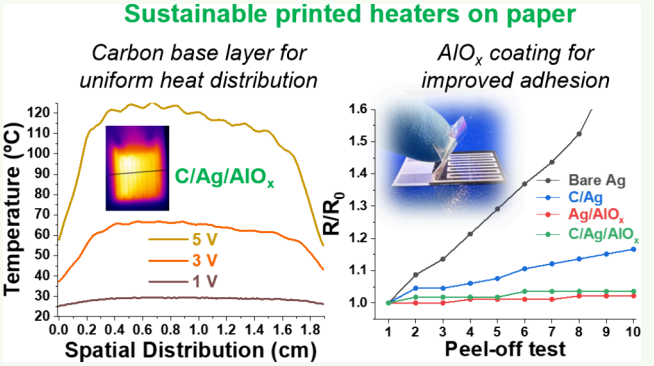

KEYWORDS: *screen printing, water-based inks, Joule heating, IR imaging, adhesion, wearables*

INTRODUCTION

The development of thin-film, flexible heaters has garnered significant attention due to their potential in diverse applications (smart windows, deicers, defoggers, thermotherapy pads, and sensors) for different industrial sectors (transport, buildings, healthcare, and sport).[1−5] Thermal therapy, a widely used treatment for conditions like osteoarthritis and carpal tunnel syndrome, benefits from controlled heating to enhance tissue temperature, improve blood flow, and reduce muscle stiffness and inflammation.[6,7] Advancements in printed electronics offer new avenues for creating cost-effective, scalable, and sustainable heaters that can be seamlessly integrated into wearable and medical devices.[8]

Several techniques have been employed to develop printed heaters, including inkjet printing or spray coating.[9−11] However, screen printing is preferred for its versatility in large-scale manufacturing and compatibility with roll-to-roll (R2R) processes.[12] Among the available conductive materials, such as silver nanowires, graphene, carbon, and MXenes,[13−18] silver-based inks are particularly promising due to their high conductivity and chemical stability.[19] However, traditional silver inks often rely on harmful organic solvents, raising environmental concerns.[20] This challenge has led to the development of water-based silver inks, which provide a more sustainable alternative.[21,22] Furthermore, screen-printed heaters have also been developed on biodegradable substrates like paper.[17,23−25] These materials are aligned with the United Nations' Sustainable Development Goals (SDGs), promoting greener manufacturing methods and dealing with the constantly increasing problem of e-waste.[26]

Flexible printed heaters face challenges in ensuring uniform heat distribution, particularly when integrated into larger devices. Previous studies have demonstrated that heaters using

Received: February 12, 2025
Revised: April 26, 2025
Accepted: April 28, 2025
Published: May 25, 2025

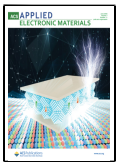

Table 1. Comparison between Screen-Printed Heaters on Paper Substrates[a]

ink (solvent), substrate, ref	electrical properties	T_{steady} (°C)	volt. (V)	power (W/cm^2)	stability tests	device demo	T_{steady}, voltage, size, cost
carbon pigment (water-based), photocopy paper[25]	146 Ω	54	15	N/A	0.3 h 15−0 V	microfluidics platform	37 °C, N/A, 1.4 × 1.5 cm^2, 10¢ (0.60 €) per heater
Cu@Ni RSNWs (water-based), photocopy paper[23]	1.9 Ω/sq	172.8	6	0.62	1.5 h 2−6 V	heating wristband	50.4 °C, 3 V, 1.3 × 11 cm^2 (each one 1 × 1.3 cm^2), N/A
MXene/xanthan gum (water-based), photographic paper[17]	4.8 × 10^4 S/m	130.8	4	1.1 (0.55 A, 1 × 2 cm^2)	6 h cst 2.5 V	deicing block	2.5 V (19 min), 1 × 2 cm^2, N/A
Ag/C/AlO$_x$ (water-based), office paper (this work)	13.1 Ω	120	5	0.75 (0.36 A, 1.5 × 1.6 cm^2)	6 h 5−0 V	heating bandage	50 °C, 3.5 V, 2 × 3.6 cm^2, 0.20 € per heater

[a]Power density values are either reported in the cited works or estimated based on available data. The T_{steady} values refer to the maximum steady-state temperatures reached under the same, reported applied voltage (volt.), while the final column presents performance data for the demonstrated devices, which may have been operated under different voltage conditions. N/A = not available.

carbon-based conductive materials, continuously deposited over a substrate, provide good heat uniformity compared to approaches involving resistor patterns of more conductive materials.[18] Among investigations of screen printed heaters on paper, Atabakhsh et al. were the first to implement a low-cost temperature control system based on a resistive heater for paper-based microfluidics.[25] However, due to carbon's high electrical resistance, these heaters required a high applied voltage to reach target temperatures, such as 54 °C under 15 V. Furthermore, Liu et al. developed screen-printed heaters on paper using copper−nickel rose-stem nanowires (Cu@Ni RSNWs) in a water-based ink and integrated an array of heaters in a wristband.[23] Each heater achieved 50.4 °C under a low voltage of 3 V (10 × 13 mm^2 per heater), but the temperature between the heaters in the wristband was significantly lower. Finally, Wu et al. fabricated screen-printed heaters on paper using MXenes/xanthan gum water-based ink. Their heaters reached a high steady-state temperature of 130.8 °C s under a low voltage of 4 V (for 10 × 20 mm^2), and demonstrated promising deicing performance.[17] Table 1 provides a summary of the performance metrics of these screen-printed heaters on paper substrates. It is important to note that comparing the electrical and thermal properties of Joule-heating devices is not always straightforward, as variations in heater dimensions directly impact the electrical supply requirements. To aid comparability, power density values are also included when available or estimable. Additionally, the reported T_{steady} values correspond to the maximum steady-state temperatures reached at the specified applied voltage. Stability tests, such as voltage cycling, in some studies have been limited to relatively short durations. Another critical factor for successful integration into devices is durability under mechanical stress, commonly evaluated through tape adhesion tests.[27] Encapsulation with protective coatings has been identified as an efficient method to address poor adhesion and enhance the stability of conductive layers under environmental stress, as reported in studies on thin films.[28] The issues of adhesion and spatial uniformity, however, have not yet been adequately addressed in prior research on screen-printed heaters on paper.

While increasing the density of metallic resistor patterns could potentially improve thermal uniformity, such designs would require significantly more conductive ink-raising both material costs and limiting scalability. Instead, this study explores a multilayer strategy to enhance heat distribution without compromising on efficiency or sustainability. Here, we address the above issues by introducing a multilayer structure that combines highly conductive silver (Ag) for enhanced electrical performance, a carbon-based (C) layer for improved thermal distribution, and a protective aluminum oxide (AlO$_x$) coating to shield the heater from mechanical stress and environment conditions. Each layer is made of water-based ink and the multi-stack C/Ag/AlO$_x$ printed heaters are printed on a paper substrate. All designs were evaluated for electrical stability and thermal distribution using *in situ* infrared imaging. Moreover, tape adhesion and climatic chamber tests demonstrated enhanced performance of the multi-stack heater. Finally, a bandage heater serves as a demonstration of the heater's potential for thermotherapy applications, highlighting its flexibility and ability to achieve uniform heating while maintaining sustainability.

EXPERIMENTAL SECTION

Synthesis of AlO$_x$ Ink. The ink was produced in two steps. First, a binder solution was prepared by dissolving 10 wt % of hydroxypropyl cellulose (HPC, CAS 9004-64-2, Alfa Aesar) in deionized water. Then, aluminum oxide (Al$_2$O$_3$, CAS 1344-28-1, Fluka) was blended into the prepared solution with a concentration of 10 wt %. The mixture was slowly stirred at 200 rpm for 3 h to obtain a well-dispersed solution. The ink was stored in a refrigerator at 5 °C until being used.

Screen Printing. The printed heaters were fabricated using a manual, custom-made screen-printing station, inside a fume hood in ambient conditions (23.9−24.1 °C, 44−50% RH), with 120T meshes. Office paper (MultiOffice A4, 80 g/m^2) was used as the substrate for all the samples. Commercial, water-based highly conductive silver ink (Saral StretchSilver H2O 600, Saralon) was screen-printed with a double passage, using a mesh with four different resistor patterns (two different line widths and two different total lengths). The two short resistor patterns consist of 5 serpentines of 1.5 cm in height and two different line widths, 0.05 cm for the thicker (ST) and 0.05 cm for the finer (SF). The total size of the short heaters is 1.9 × 1.6 cm^2, including the side longer lines (1.9 cm), leading to two rectangular pads (0.4 × 1 cm^2). The two long resistor patterns consist of 10 serpentines of 1.5 cm in height and two different line widths same as the short patterns, 0.025 cm (LF) and 0.05 cm (LT). The total size of long heaters is 1.9 × 3.3 cm^2, including the side longer lines (1.9 cm), leading to two rectangular pads (0.4 × 1 cm^2). After the Ag ink deposition, the samples were annealed inside an oven at 100 °C for 60 min to evaporate the water and sinter the ink. For the fabrication of multi-stack heaters, commercial water-based carbon conductive ink (WBC01S, NanoPaint) was screen-printed before Ag resistors, with a double-passage, using a mesh that consists of rectangles with two different sizes. The size of each rectangular pattern is 2 × 1.9 and 2 × 3.6 cm^2, intended to cover the resistor patterns and leave uncovered the longer side lines and the contact pads. After deposition, the carbon rectangular patterns were left to dry overnight inside the fume

https://doi.org/10.1021/acsaelm.5c00305
ACS Appl. Electron. Mater. 2025, 7, 4862−4871

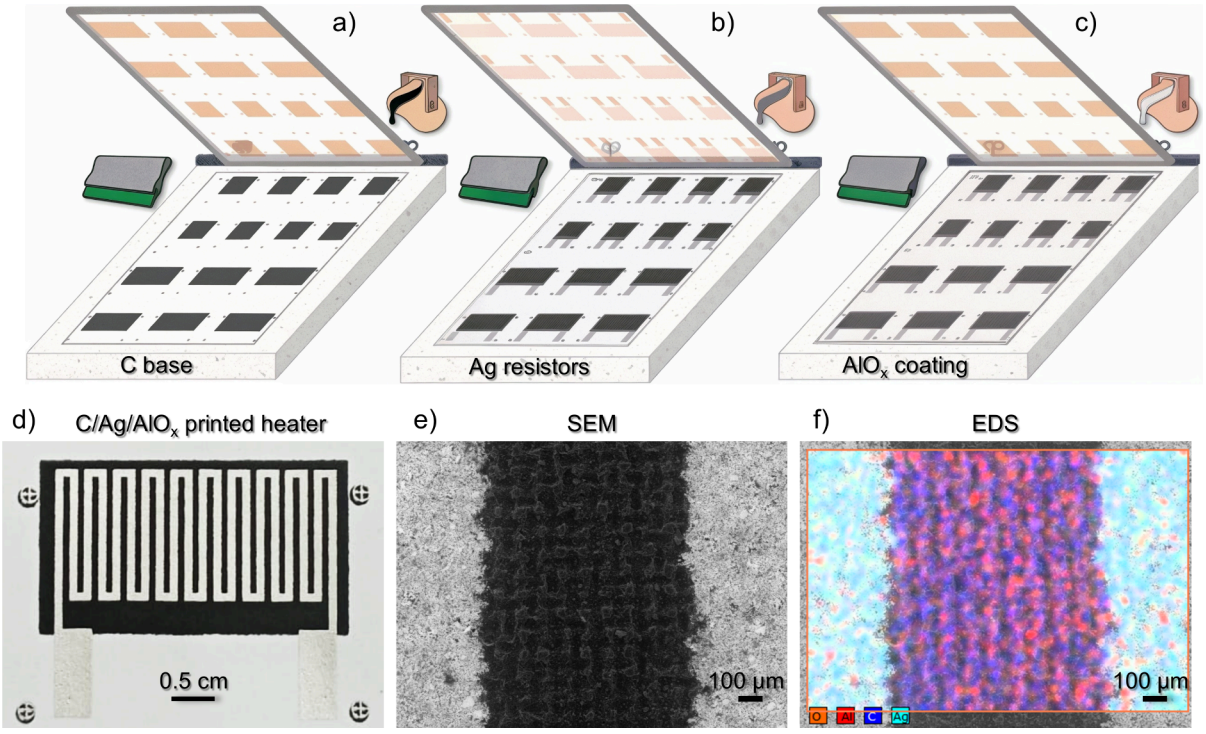

Figure 1. Fabrication and morphology of multi-stack printed heaters on paper. (a–c) Schematic representation of the multi-stack heater fabrication process using screen printing with water-based inks on a paper substrate. (a) Screen with two different rectangular sizes for printing the carbon base (C-base). (b) Screen with resistor patterns featuring varying line widths and lengths for silver (Ag) printing. (c) Same screen as in panel a used for printing the aluminum oxide (AlO_x) coating. (d) Photograph of a multi-stack heater with a long-thick resistor pattern. (e) SEM image of a multi-stack heater, clearly distinguishing the silver regions (left and right) and the carbon base (center). (f) EDS mapping of the SEM image, showing Ag (light blue), C (blue), and AlO_x (red) uniformly covering the entire sample.

hood. For the heaters coated with the metal oxide thin film, water-based in-house AlO_x ink was screen-printed with one passage on top of Ag or C/Ag heaters, using the same mesh as the one for the carbon rectangles. After deposition, the samples were annealed inside an oven at 100 °C for 30 min to evaporate the water.

Morphological, Electrical, and Thermal Characterization. Morphological characterization of the printed heaters was performed using tabletop scanning electron microscopy at 5 kV (SEM TM3030 Plus, Hitachi), equipped with an energy-dispersive spectroscopy system (EDS Quantax 70, Bruker). The electrical characterization platform included a source meter unit (SMU, Keithley 2400, Tektronix, with current compliance 1 A) and a workstation to control the SMU via Python scripts, developed in-house. This allowed the recording of the applied voltage and the measured current every 3 s, to further calculate the resistance of the printed heater during the electrical tests. Flat crocodiles with long wires were clipped directly to the rectangles of the heaters, without any ink or paste deposited on them. This method was also used for long-term stability measurements. An infrared (IR) thermal imager (Testo890) was used to monitor the surface temperature and analyze the heat spatial distribution of heat and other heating properties of the printed heaters, using IRSoft software. For a fair comparison of the generated heat, since there is a significant difference in the emissivity values between the paper and the inks, all thermal measurements were performed from the back side of the printed heaters (only the paper side) and using an emissivity of 0.9, according to the method and results presented in our recent work.[5] Moreover, an emission tape for measurements on reflective surfaces (Testo) was placed on the side of these metallic crocodiles facing the IR camera, to avoid the reflection from their surface. IR sequences were recorded every 3 s during all experiments, except the 6 h voltage cycles where a time interval of 6 s was used, limited to the maximum recording capacity of IRSoft.

Adhesion Test and Environmental Stability. For the evaluation of the inks' adhesion and mechanical durability, transparent adhesive tape (Scotch) was manually placed on top of the samples and manually peeled off. The chosen tape had a 1.9 cm width to cover the printed heaters (short thick, ST, pattern). Before the adhesion test, the samples were stuck with a double-sided adhesive tape (tesa) to a metallic base to ensure that they were fixed and flat. A new piece of tape was used for each test (in total 10 repetitions for each sample) and the electrical resistance was measured every time with a multimeter. For environmental stability, samples with small fine (SF) patterns were placed inside a climatic test chamber (WEBSeason, Weiss Technik) at 80 °C and 80% relative humidity. Before the test, long copper wires were stuck on the contact pads of the bare Ag and the Ag/AlO_x samples, using Ag ink, and were inserted through the silicone foam port plug. As for the C/Ag/AlO_x heater, it was connected directly to flat crocodile clip-long wires that had been previously inserted through the same port plug. Additional photos of the setup are presented in the Supporting Information.

Skin Bandage–Heater Fabrication. For the thermotherapy demo, a multi-stack printed heater (LF pattern) was integrated into an adhesive bandage (BAND-AID Jumbo, Johnson & Johnson). Before the attachment of these two materials, long copper wires were stuck to the contact pads of the heater using Ag ink and left dry inside the fume hood overnight. Then, a piece of double-sided adhesive tape (tesa) was stuck on the multi-stack heater side (above the AlO_x coating) and the second protective layer of the tape was removed to stick the heater on the external side of the bandage. A cross-section schematic, photos of the fabrication steps, and a video of the device during operation are presented in the Supporting Information.

RESULTS AND DISCUSSION

Fabrication and Morphological Analysis of Multi-stack Heaters. The multi-stack heaters were fabricated using a screen-printing technique with water-based inks and paper as substrate. Two custom-made 120-mesh screens were employed

https://doi.org/10.1021/acsaelm.5c00305
ACS Appl. Electron. Mater. 2025, 7, 4862–4871

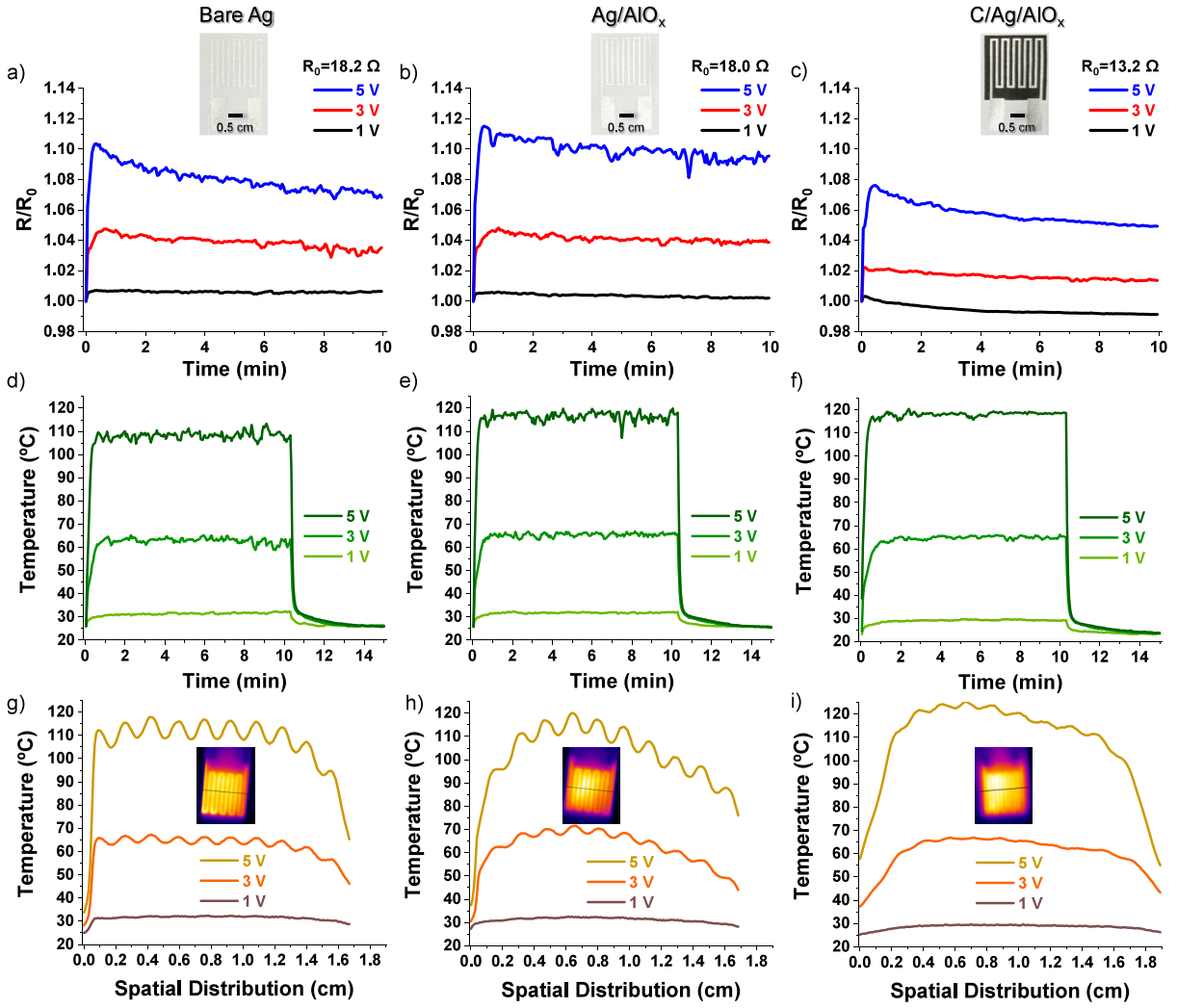

Figure 2. Electrical and thermal performance of printed heaters on paper under a constant applied voltage of 1, 3, or 5 V for 10 min, followed by cooling. The resistors presented are of the short and fine (SF) pattern. (a–c) Evolution of relative resistance (R/R_0) for the bare Ag (R_0 = 18.2 Ω), Ag/AlO_x-coated (R_0 = 18.0 Ω), and multi-stack C/Ag/AlO_x (R_0 = 13.2 Ω) heaters, respectively. Black, red, and blue lines correspond to 1, 3, and 5 V, respectively. Insets depict photos of the samples. (d–f) Temperature evolution recorded by IR imaging at a central point on the heaters for the bare Ag, Ag/AlO_x-coated, and multi-stack C/Ag/AlO_x heaters, respectively. Light green, green, and dark green lines correspond to 1, 3, and 5 V, respectively. (g–i) Spatial temperature distribution along a central line across the resistors at the midpoint of each voltage plateau for the bare Ag, Ag/AlO_x-coated, and multi-stack C/Ag/AlO_x heaters, respectively. Brown, orange, and ochre lines correspond to 1, 3, and 5 V, respectively. Insets show the IR sequence during the 5 V plateau, with black lines indicating the regions analyzed for spatial temperature distribution.

to achieve precise patterning during the multistep, full printing process. Initially, the carbon (C) base layer was printed using a screen with two differently sized rectangular patterns, as shown in Figure 1a. This layer forms a conductive foundation for the heater intended to homogenize the heat spatial distribution cost-effectively.[29] Following this, silver (Ag) resistor patterns were printed on top of the carbon base. The resistor patterns were designed with varying line widths and lengths to tailor the electrical resistance and, consequently, the heating performance (Figure 1b). The final layer involved printing an aluminum oxide (AlO_x) coating using the same screen as the carbon layer (Figure 1c). This insulating layer was intended to ensure the durability of the device during operation and protection against aging and environmental stress, thanks to the properties of AlO_x-based thin films.[30] The C and Ag water-based inks are commercial and the AlO_x is developed in-house. More details about the inks, screens, printing process, and post-annealing can be found in the Experimental Section.

Figure 1d shows a photo of a completed multi-stack heater with a long-thick pattern (LT), demonstrating the layered structure. Morphological characterization was performed using scanning electron microscopy (SEM), which revealed the distinct separation between the carbon and silver layers (Figure 1e). In this image, silver appears on the left and right sides, while the carbon base occupies the middle section. The AlO_x coating is more difficult to distinguish here, but as presented in additional SEM images of Figure S1, the coating difference is much more visible when comparing Ag bare and AlO_x coated samples (panels a–c and d–f of Figure S1, respectively), as well as the interface between the AlO_x coated and bare paper (panels g–i of Figure S1). AlO_x particles can be observed and there is also a difference in the image contrast that can be attributed to the insulating nature of the coating. Moreover, energy-dispersive X-ray spectroscopy (EDS) was used for elemental mapping of the heater (Figure 1f and panels j–l of Figure S1). The EDS mappings confirm the presence of silver

https://doi.org/10.1021/acsaelm.5c00305
ACS Appl. Electron. Mater. 2025, 7, 4862–4871

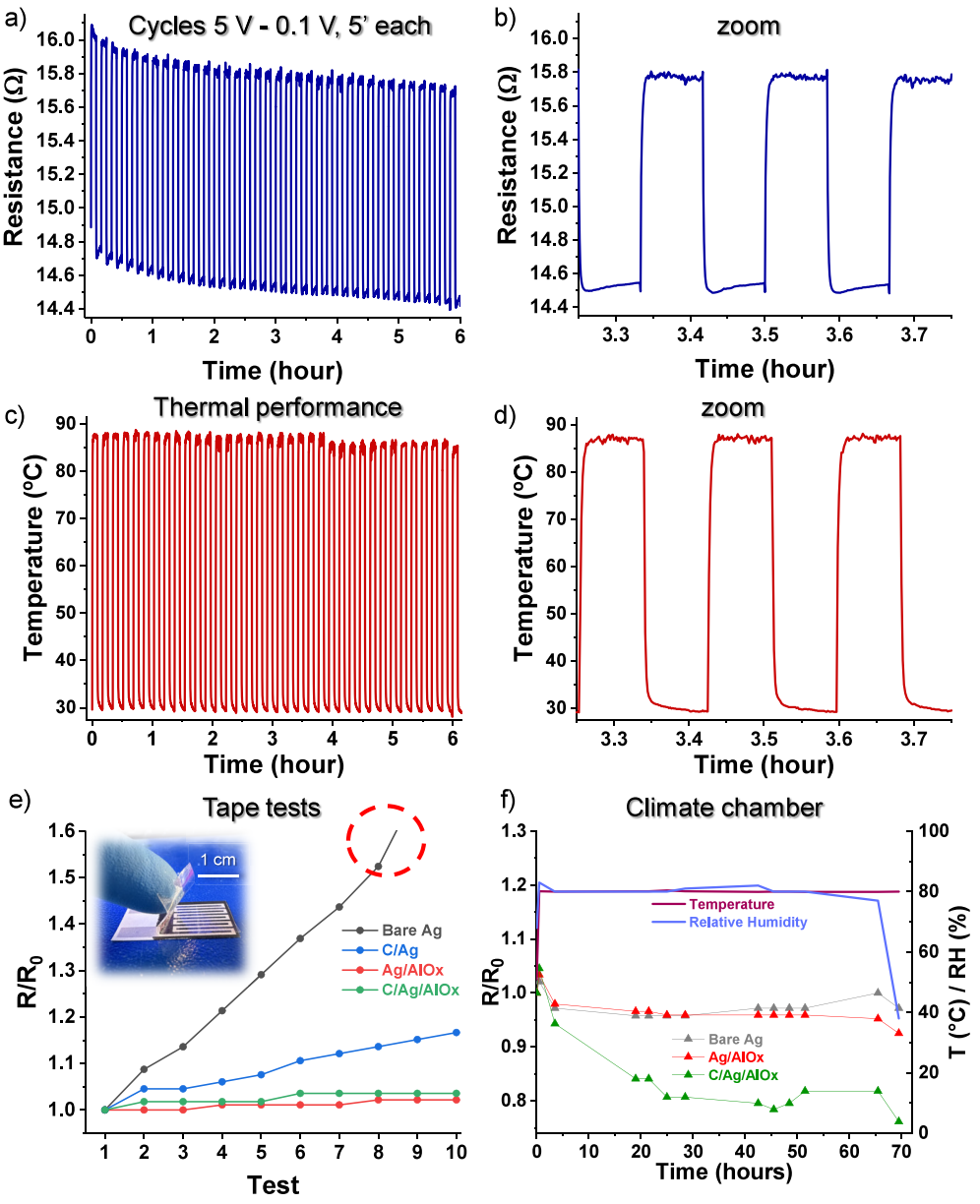

Figure 3. Printed heaters on paper: stability under electrical, mechanical, and environmental stress. (a and b) Voltage cycling of 5 and 0.1 V applied alternately for 5 min over 6 h on a multi-stack C/Ag/AlO_x heater. (a) Resistance evolution. (b) Zoomed-in view of three cycles in the middle of the experiment. (c) Temperature evolution at a central point of the heater. (d) Zoomed-in temperature profile corresponding to the cycles shown in panel b. (e) Tape adhesion tests for bare Ag (gray line with dots), C/Ag (blue line with dots), Ag/AlO_x (red line with dots), and C/Ag/AlO_x multi-stack (green line with dots) heaters. Relative resistance change (R/R_0) measured after each tape peel-off, repeated 10 times. Bare Ag exhibited a resistance increase to infinity after the 9th peel. (Inset) Multi-stack heater with tape applied before removal. (f) Environmental stress in a climate chamber (80 °C, 80% RH). Relative resistance change (R/R_0) measured *in situ* at regular intervals using long wires extending outside the chamber for bare Ag (gray line with dots), Ag/AlO_x coated (red line with dots), and C/Ag/AlO_x multi-stack (green line with dots) heaters. Continuous dark red and violet lines indicate the recorded temperature and relative humidity, respectively.

(Ag) in the outer regions (light blue) and carbon (C) in the middle (blue). As can be observed more clearly in Figure S1j, C is also present below Ag, although not readily visible in the EDS mapping, apart from regions where small pores in Ag could be found, owing to the strong signal arising from the thick Ag-printed layer. The mapping of aluminum (Al) in Figure S1l demonstrates that the AlO_x coating covers the entire surface (red).

Ensuring uniform deposition of the Ag ink is critical to achieving reproducible electrical resistance and consistent heater performance for each pattern. For this, a statistical analysis of the reproducibility of the manual screen-printing has been performed, as presented in Figure S2. Five groups of the four different heater patterns were deposited on paper (design and photo in panels a and b of Figure S2), giving three samples of the same pattern in each group. The mean values of the electrical resistance as plotted for each pattern (panels c–f of Figure S2) confirm that the screen-printing process is very reproducible. Furthermore, the electrical resistance values were plotted by the position of the sample in each heater pattern and group (panels g–j of Figure S2). The same tendency is observed in all cases: the right samples demonstrate a little

https://doi.org/10.1021/acsaelm.5c00305
ACS Appl. Electron. Mater. 2025, 7, 4862−4871

lower electrical resistance than the left and middle ones. This can be explained considering that higher force is applied on the edges of the squeegee, especially the right, during the manual screen-printing, because of the placement of the left and right hands of the right-hand user that performed the deposition.

Electrical−Thermal Performance: Heat Spatial Distribution and Impact of Carbon Base. After fabricating the printed heaters on paper, their electrical and thermal performance was evaluated through a series of voltage plateaus applied at 1, 3, and 5 V for 10 min each. Each voltage application was followed by a 5 min cooling period to assess the heater's ability to return to baseline conditions. *In situ* monitoring of the Joule heating effect was performed using IR imaging on the substrate side of the heaters to capture both temporal and spatial thermal responses accurately. A photo of the measurement setup is presented in Figure S3j, including a photo of the crocodiles clipped to the heater and the emission tape covering them. This setup enabled detailed analysis of resistance changes over time, temperature evolution at specific points, and heat distribution across the heaters. Three heater configurations were studied: bare silver (Ag), silver coated with aluminum oxide (Ag/AlO_x), and the multi-stack structure comprising a carbon base, silver, and an aluminum oxide coating ($C/Ag/AlO_x$). Figure 2 summarizes the results for heaters with a short and fine (SF) resistor pattern, while additional data for other patterns, including short-thick (ST), long-fine (LF), and long-thick (LT), are provided in the Supporting Information.

Panels a−c of Figure 2 illustrate the evolution of electrical resistance over time for the three heater types, with insets showing photos of each sample. The black, red, and blue lines correspond to applied voltages of 1, 3, and 5 V, respectively. The initial resistance values were approximately 18 Ω for both the bare Ag and Ag/AlO_x-coated heaters, while the $C/Ag/AlO_x$ multi-stack showed a lower resistance of 13 Ω. The carbon ink's contribution to electrical percolation, despite its lower conductivity compared to silver, explains this difference. All heaters exhibited minimal resistance changes at 1 and 3 V. The initial resistance increase during heating is attributed to the temperature dependence of the materials' resistivity (TCR).[2] Moreover, at 5 V, a slight resistance decrease was noted, likely due to further sintering driven by higher Joule heating. The $C/Ag/AlO_x$ multi-stack (Figure 2c) demonstrated the most stable resistance profiles across all conditions.

The temperature evolution, monitored at a central point on the heater, is presented in panels d−f of Figure 2. The light green, green, and dark green lines represent 1, 3, and 5 V, respectively. All heaters demonstrated rapid temperature rise, peaking at approximately 120 °C at 5 V. The temperature range remains within the operational limits of the paper substrate without risking degradation. A swift cooldown was observed once the voltage was removed. Fluctuations of approximately ±5 °C were observed in the bare Ag (Figure 2d) and Ag/AlO_x-coated (Figure 2e) heaters during the steady-state temperature phase, likely due to localized heat dissipation challenges and substrate heterogeneities. In contrast, the $C/Ag/AlO_x$ multi-stack heater (Figure 2f) achieved more uniform heating maintaining steady temperatures across all voltage levels.

Panels g−i of Figure 2 provide insights into the spatial heat distribution along a central line across the heaters, captured at the midpoint of each voltage plateau. The brown, orange, and ochre lines correspond to 1, 3, and 5 V, respectively. At 1 V, the Joule heating was minimal, resulting in negligible fluctuations. At 3 and 5 V, however, the bare Ag heater (Figure 2g) exhibited a temperature gradient of approximately 5 °C at 3 V and 10 °C at 5 V, between the silver lines and the cooler regions in the paper, indicating uneven heat dissipation. The Ag/AlO_x-coated heater (Figure 2h) showed similar variations. Notably, the multi-stack $C/Ag/AlO_x$ heater (Figure 2i) demonstrated superior thermal uniformity with fluctuations of approximately ±1 °C at 3 V and ±3 °C at 5 V. This performance is attributed to the combined effects of the carbon base's thermal conduction and its synergy with the silver resistor. IR images during the 5 V plateau (insets in panels g−i of Figure 2) highlight thermal profiles, with the black lines indicating the regions analyzed for spatial temperature distribution. The less distinct resistor pattern observed in the inset IR image of Figure 2i is due to the significantly improved heat uniformity achieved by the $C/Ag/AlO_x$ heater. These insights underscore the importance of accurate thermal mapping in evaluating heater performance. Overall, the results, consistent across all resistor patterns as presented in Figures S3, S4, and S5, confirm that the multi-stack $C/Ag/AlO_x$ heaters consistently exhibited enhanced electrical stability and superior thermal uniformity compared to the other configurations, highlighting their potential for sustainable, flexible heater applications.

Stability under Electrical, Mechanical, and Environmental Stress: Impact of AlO_x Coating. The printed heaters were subjected to a series of stability and durability tests, including prolonged electrical cycling, mechanical adhesion tests, and environmental exposure. First, voltage cycling tests were performed on a $C/Ag/AlO_x$ multi-stack heater with a long thin (LF) pattern. The heater alternated between 5 and 0.1 V in 5 min intervals for 6 continuous hours. Figure 3a shows the evolution of resistance (Figure 3b zoomed in on three cycles from the middle of the experiment), which gradually decreased over time due to further sintering induced by Joule heating. Results for the bare Ag and Ag/AlO_x-coated heaters are provided in the Supporting Information, showing stable and reproducible performance across all cycles. Temperature measurements, taken at a central point on the heater (Figure 3c), fluctuated between 30 °C (off state) and nearly 90 °C (on state), reflecting rapid heating and cooling. For example, these rates calculated from a zoom in 3.5 h (Figure 3d) are for heating 60 °C/min to reach the maximum temperature (T_{max} = 87.3 °C from 29.2 °C), 164 °C/min to reach 90% of T_{max} (78.5 °C), and for cooling −31.6 °C/min to drop to 30.2 °C. It should be noted that it takes another 2.7 min to reach 29.2 °C from 30.2 °C, due to the elevated room temperature when the experiment was conducted. Moreover, the results of bare Ag and Ag/AlO_x-coated samples, presented in Figure S6, demonstrate electrical and thermal performance of similar stability.

Adhesion tests were performed using a standardized tape-peeling method as described in the Experimental Section. Four configurations were tested: bare Ag, C/Ag, Ag/AlO_x, and $C/Ag/AlO_x$ multi-stack heaters, with a small thick (ST) pattern. As shown in Figure 3e, the bare Ag heater exhibited a significant increase in resistance after the ninth peel, as parts of the silver and underlying paper were damaged, ultimately resulting in a complete loss of electrical percolation. The C/Ag configuration, without AlO_x coating, was included in this test to assess the contribution of the carbon base to adhesion. This configuration showed a moderate resistance increase of 15%,

https://doi.org/10.1021/acsaelm.5c00305
ACS Appl. Electron. Mater. 2025, 7, 4862−4871

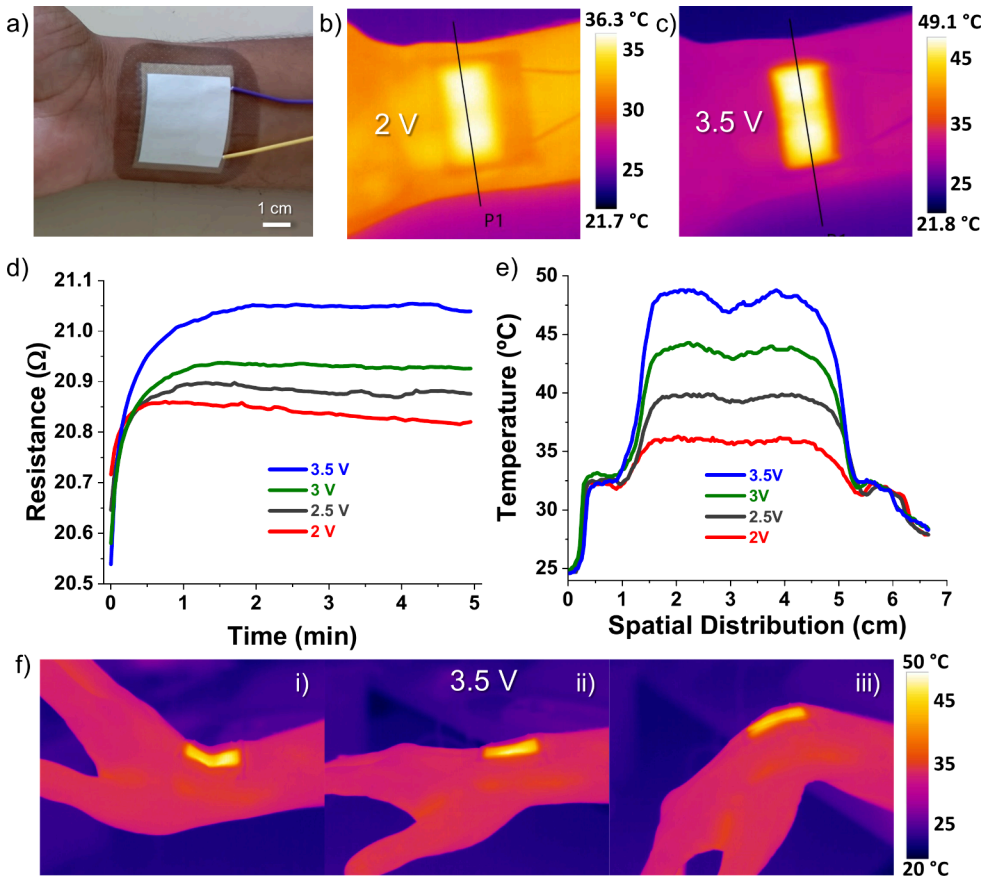

Figure 4. Printed heater embedded on a bandage for thermotherapy. A multi-stack printed heater with a long fine (LF) pattern is stuck to a bandage using double-sided tape. (a) Photograph of the device placed on the lower part of the volar side of the wrist, with wires leading to a power source. (b and c) IR images of the device during application of 2 V (b) and 3.5 V (c). (d) Resistance evolution over 5 min at different voltage plateaus: 2, 2.5, 3, and 3.5 V. (e) Spatial temperature distribution along a central line across the device at the midpoint of each voltage plateau. (f) IR images of the device on the dorsal side of the wrist at 3.5 V, showing different wrist positions: (i) bent upward, (ii) aligned with the hand, and (iii) bent downward.

outperforming the bare Ag heater and indicating that the carbon base positively impacts adhesion, likely because it covers the paper substrate. The best performance was observed for the Ag/AlO_x and C/Ag/AlO_x heaters, which maintained nearly unchanged electrical resistance throughout the test, demonstrating superior adhesion and mechanical robustness provided by the metal oxide coating. Notable, while the AlO_x coating may be partially removed during the tape tests, it serves as a protective barrier, preventing damage to the underlying conductive layers. Additional photos of all the samples during the tape tests are provided in Figure S7, where the beginning of the damage of the bare Ag heater after the fifth peel cycle is clearly visible (Figure S7a-ii and iii).

In addition, heaters with a SF pattern were placed in a climatic test chamber at 80 °C and 80% relative humidity (RH) for nearly 3 days of continuous testing, during which electrical resistance was measured *in situ* every few hours (details on the mounting process in the Experimental Section and panels a and b of Figure S8). *In situ* resistance measurements (Figure 3f) showed stable performance for all samples, with the multi-stack heaters exhibiting even slight decrease in resistance. Multimeter readings taken before and after the test (Figure S8c) confirmed that the heaters remained intact, with the electrical resistance decreasing by approximately 30% across all configurations. The stability can be attributed to the water-resistant properties of the three inks, while the decrease in electrical resistance may be associated with further sintering of the Ag particles under the temperature and humidity conditions, resembling capillary-force-induced cold welding phenomena previously observed for Ag nanowires.[31,32] Such a possibility would be interesting to explore in the future for moisture-assisted, low-temperature sintering of printed ink particles.

The *in situ* fluctuations for the bare Ag and AlO_x-coated heaters can be attributed to measurement artifacts caused by wiring damage, as revealed at the end of the climate chamber test (Figure S8d). This is noteworthy because the photos show that the copper wires attached to the bare and AlO_x-coated heaters were oxidized, likely due to the presence of moisture. This oxidation did not affect the stainless crocodile clips, already mounted to the chamber, and directly connected to the multi-stack C/Ag/AlO_x. For this configuration, the resistance decrease was recorded both *in situ* and after the climate chamber test. A long-term test over 30 days under the same extreme conditions (80 °C and 80% RH) is recommended as a future step to thoroughly evaluate long-term durability. Finally, resistance values of two samples from each configuration (bare Ag, AlO_x-coated, and C/Ag/AlO_x) were measured by multimeter over 4.5 months under ambient conditions, demonstrating high stability (Figure S9).

Demo of Printed Heater Embedded on a Bandage for Thermotherapy. To explore wearable applications, a multi-

https://doi.org/10.1021/acsaelm.5c00305
ACS Appl. Electron. Mater. 2025, 7, 4862−4871

stack C/Ag/AlO_x printed heater with a long fine (LF) pattern was embedded in a bandage using double-sided tape, ensuring flexibility and comfort. Figure 4a shows the heater positioned on the volar side of the wrist, with wires exiting the bandage for connection to a power source. More fabrication details and photos can be found in the Experimental Section and Figure S10, respectively. Furthermore, an approximate calculation of the materials cost is less than 0.20 € per heater, showing its cost-efficiency. The table in Figure S11 presents the calculation of the mass of the three deposited inks on paper by measuring the samples before and after screen-printing of two passages (photos in Figure S11) and the estimation of the cost based on the value of the commercial inks (C and Ag) and the in-house AlO_x. Considering, the commercial bandage and copper wires cost, the heater-bandage device costs approximately 0.80 €. It is worth mentioning that this cost can be even lower if all the inks were prepared in-house, as well as in the case of mass production.

Thermal performance was evaluated at applied voltages between 2 and 3.5 V. Panels b and c of Figure 4 present IR images of the heater at these voltages, highlighting uniform heating in the contact area. The highest recorded temperature reached approximately 50 °C on the upper side of the heater, ensuring a lower and safer temperature at the skin interface due to the temperature gradient across the heater, bandage, and skin. The estimated power density, given the heater's size, is 7.2 cm^2, and its electrical resistance 21 Ω at 3.5 V, is approximately 0.08 W/cm^2. The black lines on the IR images indicate the paths used to measure spatial temperature distribution. An IR Video S1 during testing at 3.5 V is available in the Supporting Information.

Electrical stability was assessed by applying successive voltage plateaus of 2, 2.5, 3, and 3.5 V for 5 min each. Figure 4d shows the evolution of electrical resistance, indicating stable and reproducible performance throughout the test. Corresponding spatial temperature profiles along a central line at the midpoint of each voltage plateau are shown in Figure 4e, confirming consistent heat dissipation.

Throughout the test, the user was periodically asked about comfort levels at each voltage plateau. At 3.5 V, the heater provided sufficient warmth while remaining within safe and comfortable limits. Flexibility was further demonstrated by attaching the heater to the dorsal side of the wrist, with IR images captured under 3.5 V in different wrist positions: bent upward (Figure 4f-i), aligned with the hand (Figure 4f-ii), and bent downward (Figure 4f-iii). In a nutshell, the multi-stack heater was embedded in a commercial bandage in a facile way and maintained uniform heating in all wrist positions, demonstrating its adaptability and potential for wearable thermotherapy applications.

CONCLUSION

The multi-stack heater, fabricated using water-based inks on a biodegradable paper substrate, demonstrated excellent electrical and thermal performance. At 5 V, the C/Ag/AlO_x heater achieved a peak temperature of approximately 120 °C, with spatial temperature fluctuations within ±3 °C, showing superior thermal uniformity compared to bare Ag and Ag/AlO_x heaters, which exhibited temperature gradients up to 10 °C. The carbon base, cost-efficient compared to silver, effectively addresses heat inhomogeneity, ensuring thermal consistency without compromising performance. All heater configurations exhibited robust durability during 6 h of 5 V cycling, with minimal resistance changes during environmental stability tests under 80 °C and 80% relative humidity, further validating the heater's robustness. In mechanical adhesion tests, the C/Ag/AlO_x heater maintained nearly unchanged resistance after 10 peel cycles, demonstrating excellent mechanical stability, attributed to the AlO_x coating, which significantly mitigates mechanical scratching. In wearable applications, the multi-stack heater, easily embedded in a commercial bandage and attached to the skin, reached a maximum temperature of 50 °C at 3.5 V, with a power density of 0.08 W/cm^2, and maintained performance under wrist bending. Moreover, the materials cost is estimated at 0.20 € per heater and 0.80 € per device. These results highlight the potential of multi-stack printed heaters for sustainable, flexible, cost-efficient, and eco-friendly applications, paving the way for innovations in wearable thermotherapy and beyond. Future work will focus on long-term aging tests and further characterization and modeling of the mechanisms behind the electrical and thermal distribution of the heater to optimize its performance. In parallel, exploring the use of recycled inks could offer an additional pathway toward further reducing the environmental footprint of such printed devices.

ASSOCIATED CONTENT

Supporting Information

The Supporting Information is available free of charge at https://pubs.acs.org/doi/10.1021/acsaelm.5c00305.

IR recording of the multi-stack printed heater in operation at 3.5 V, applied on the wrist (Video S1) (MPG)

Additional data on the fabrication, characterization, and performance of the printed heaters: SEM images of bare Ag and Ag/AlO_x coated printed heaters and EDS mappings of the multi-stack printed heater on paper substrate (Figure S1), statistical analysis of the reproducibility of manual screen-printing deposition (Figure S2), electrical−thermal performance of various heater geometries, including short-thick, long-fine, and long-thick configurations, along with photos of the experimental setup, photos of the samples and IR images under applied voltage (Figures S3−S5), stability of bare Ag and Ag/AlO_x-coated heaters under cyclic voltage operation (0.1−5 V) for 6 h (Figure S6), photos of the printed heaters during the tape adhesion test (Figure S7), images of the climate chamber setup and a summary table of electrical resistance values before and after the 72 h test at 80 °C and 80% RH (Figure S8), electrical resistance evolution of printed heaters stored under ambient conditions over 4.5 months (Figure S9), and design and application of a multi-stack printed heater on a bandage, including schematic and fabrication steps (Figure S10) (PDF)

AUTHOR INFORMATION

Corresponding Authors

Dorina T. Papanastasiou − *CENIMAT|i3N, Department of Materials Science, School of Science and Technology, NOVA University Lisbon and CEMOP/UNINOVA, 2829-516 Caparica, Portugal;* orcid.org/0000-0001-8471-8789; Email: t.papanastasiou@fct.unl.pt

Emanuel Carlos − *CENIMAT|i3N, Department of Materials Science, School of Science and Technology, NOVA University*

https://doi.org/10.1021/acsaelm.5c00305
ACS Appl. Electron. Mater. 2025, 7, 4862−4871

Lisbon and CEMOP/UNINOVA, 2829-516 Caparica, Portugal; orcid.org/0000-0002-5956-5757;
Email: e.carlos@fct.unl.pt

Authors

Daniel Morais − *CENIMAT|i3N, Department of Materials Science, School of Science and Technology, NOVA University Lisbon and CEMOP/UNINOVA, 2829-516 Caparica, Portugal*

Raquel Azevedo Martins − *CENIMAT|i3N, Department of Materials Science, School of Science and Technology, NOVA University Lisbon and CEMOP/UNINOVA, 2829-516 Caparica, Portugal*

Elvira Fortunato − *CENIMAT|i3N, Department of Materials Science, School of Science and Technology, NOVA University Lisbon and CEMOP/UNINOVA, 2829-516 Caparica, Portugal*

Rodrigo Martins − *CENIMAT|i3N, Department of Materials Science, School of Science and Technology, NOVA University Lisbon and CEMOP/UNINOVA, 2829-516 Caparica, Portugal*

Pedro Barquinha − *CENIMAT|i3N, Department of Materials Science, School of Science and Technology, NOVA University Lisbon and CEMOP/UNINOVA, 2829-516 Caparica, Portugal;* orcid.org/0000-0002-5446-2759

Complete contact information is available at:
https://pubs.acs.org/10.1021/acsaelm.5c00305

Notes

The authors declare no competing financial interest.

■ ACKNOWLEDGMENTS

This work was financed by national funds from Fundação para a Ciência e a Tecnologia, I.P. (FCT) in the scope of the Projects LA/P/0037/2020, UIDP/50025/2020, and UIDB/50025/2020 of the Associate Laboratory Institute of Nanostructures, Nanomodelling and Nanofabrication (i3N). Also, this work was performed within the framework of Plano de Recuperação e Resiliência (PRR) Projects "R2U Technologies|Modular Systems" (C644876810-00000019) and "Agenda Be.Neutral" (C625244769-00462300). The authors express their gratitude to Dr. Alexandra Gonçalves for her invaluable laboratory assistance. Special thanks also go to Dr. Miguel Alexandre, Aníbal Costa, and Francisco Janeiro for their contributions to developing the Python scripts used in controlling the electrical measurements.

■ REFERENCES

(1) Liu, Q.; Tian, B.; Liang, J.; Wu, W. Recent Advances in Printed Flexible Heaters for Portable and Wearable Thermal Management. *Mater. Horiz.* **2021**.

(2) Papanastasiou, D. T.; Schultheiss, A.; Muñoz-Rojas, D.; Celle, C.; Carella, A.; Simonato, J.-P.; Bellet, D. Transparent Heaters: A Review. *Adv. Funct. Mater.* **2020**, *30* (21), 1910225.

(3) Fang, S.; Wang, R.; Ni, H.; Liu, H.; Liu, L. A Review of Flexible Electric Heating Element and Electric Heating Garments. *J. Ind. Text.* **2022**, *51* (1_suppl), 101S−136S.

(4) Carlos, E.; Martins, R.; Fortunato, E.; Branquinho, R. Solution Combustion Synthesis: Towards a Sustainable Approach for Metal Oxides. *Chem. - Eur. J.* **2020**, *26* (42), 9099−9125.

(5) Papanastasiou, D. T.; Costa, A.; Janeiro, F.; Barquinha, P.; Carlos, E. Paper-Based Printed Heaters for Low-Cost Comfort Applications. *Proceedings of the 6th IEEE International Flexible Electronics Technology Conference (IFETC 2024)*; Bologna, Italy, Sept 15−18, 2024; DOI: 10.1109/IFETC61155.2024.10771860.

(6) Shukla, D.; Liu, Y.; Zhu, Y. Eco-Friendly Screen Printing of Silver Nanowires for Flexible and Stretchable Electronics. *Nanoscale* **2023**, *15* (6), 2767−2778.

(7) Pillai, P. S.; Athira, B. S.; Varghese, H.; Agarwal, S.; Kumar, B.; Alagirusamy, R.; Das, A.; Surendran, K. P.; Chandran, A. A Resistive Ink Based All-Printed Fabric Heater Integrated Wearable Thermotherapy Device. *J. Mater. Sci. Mater. Electron.* **2023**, *34* (16), 1261.

(8) Wei, R.; Li, H.; Chen, Z.; Hua, Q.; Shen, G.; Jiang, K. Revolutionizing Wearable Technology: Advanced Fabrication Techniques for Body-Conformable Electronics. *npj Flex. Electron.* **2024**, *8* (1), 83.

(9) Mitra, D.; Thalheim, R.; Zichner, R. Inkjet Printed Heating Elements Based on Nanoparticle Silver Ink with Adjustable Temperature Distribution for Flexible Applications. *Phys. Status Solidi A* **2021**, *218* (17), 2100257.

(10) Barmpakos, D.; Belessi, V.; Xanthopoulos, N.; Krontiras, C. A.; Kaltsas, G. Flexible Inkjet-Printed Heaters Utilizing Graphene-Based Inks. *Sensors* **2022**, *22* (3), 1173.

(11) Khadka, A.; Kim, B.-Y.; Park, C.; Lim, W.; Aldalbahi, A.; Periyasami, G.; Joshi, B.; Yoon, S. S. Eco-Friendly Cellulose Wearable Heaters Using Korean Traditional Han Paper Coated with Graphene Nanosheets via Binder-Free Supersonic Spraying. *Phys. Fluids* **2023**, *35* (5), 057106.

(12) Suresh, R. R.; Lakshmanakumar, M.; Arockia Jayalatha, J. B. B.; Rajan, K. S.; Sethuraman, S.; Krishnan, U. M.; Rayappan, J. B. B. Fabrication of Screen-Printed Electrodes: Opportunities and Challenges. *J. Mater. Sci.* **2021**, *56* (15), 8951−9006.

(13) Zhang, D.; Liu, L.; Leng, J.; Liu, Y. Ultra-Light Release Device Integrated with Screen-Printed Heaters for CubeSat's Deployable Solar Arrays. *Compos. Struct.* **2020**, *232*, 111561.

(14) Zhang, Y.; Ren, H.; Chen, H.; Chen, Q.; Jin, L.; Peng, W.; Xin, S.; Bai, Y. Cotton Fabrics Decorated with Conductive Graphene Nanosheet Inks for Flexible Wearable Heaters and Strain Sensors. *ACS Appl. Nano Mater.* **2021**, *4* (9), 9709−9720.

(15) He, X.; Shen, G.; Xu, R.; Yang, W.; Zhang, C.; Liu, Z.; Chen, B.; Liu, J.; Song, M. Hexagonal and Square Patterned Silver Nanowires/PEDOT:PSS Composite Grids by Screen Printing for Uniformly Transparent Heaters. *Polymers* **2019**, *11* (3), 468.

(16) Liu, Y.; Ma, X.; Zhang, H.; Sun, J.; Qian, J.; Wang, X. Large-Scale Production of Electrothermal Films with GNSs/CNTs/CB Three-Dimensional Structure Ink by Screen Printing. *ACS Appl. Electron. Mater.* **2022**, *4* (2), 814−822.

(17) Wu, H.; Xie, Y.; Ma, Y.; Zhang, B.; Xia, B.; Zhang, P.; Qian, W.; He, D.; Zhang, X.; Li, B.; Nan, C. Aqueous MXene/Xanthan Gum Hybrid Inks for Screen-Printing Electromagnetic Shielding, Joule Heater, and Piezoresistive Sensor. *Small* **2022**, *18* (16), 2107087.

(18) Claypole, A.; Claypole, J.; Bezodis, N.; Kilduff, L.; Gethin, D.; Claypole, T. Printed Nanocarbon Heaters for Stretchable Sport and Leisure Garments. *Materials* **2022**, *15* (2), 573.

(19) Martins, P.; Pereira, N.; Lima, A. C.; Garcia, A.; Mendes-Filipe, C.; Policia, R.; Correia, V.; Lanceros-Mendez, S. Advances in Printing and Electronics: From Engagement to Commitment. *Adv. Funct. Mater.* **2023**, *33* (16), 2213744.

(20) Sanchez-Duenas, L.; Gomez, E.; Larrañaga, M.; Blanco, M.; Goitandia, A. M.; Aranzabe, E.; Vilas-Vilela, J. L. A Review on Sustainable Inks for Printed Electronics: Materials for Conductive, Dielectric and Piezoelectric Sustainable Inks. *Materials* **2023**, *16* (11), 3940.

(21) Jia, L.-C.; Zhou, C.-G.; Sun, W.-J.; Xu, L.; Yan, D.-X.; Li, Z.-M. Water-Based Conductive Ink for Highly Efficient Electromagnetic Interference Shielding Coating. *Chem. Eng. J.* **2020**, *384*, 123368.

(22) Ibrahim, N.; Akindoyo, J. O.; Mariatti, M. Recent Development in Silver-Based Ink for Flexible Electronics. *J. Sci. Adv. Mater. Devices* **2022**, *7* (1), 100395.

(23) Liu, Q.; Tian, B.; Luo, C.; Liang, J.; Wu, W. Printed Flexible Heaters-Based Thermotherapy Platform for Multiduty Thermal Management. *Adv. Mater. Technol.* **2020**, *5* (8), 2000278.

(24) Sadi, Md. S.; Yang, M.; Luo, L.; Cheng, D.; Cai, G.; Wang, X. Direct Screen Printing of Single-Faced Conductive Cotton Fabrics for Strain Sensing, Electrical Heating and Color Changing. *Cellulose* **2019**, *26* (10), 6179−6188.
(25) Atabakhsh, S.; Latifi Namin, Z.; Jafarabadi Ashtiani, S. Paper-Based Resistive Heater with Accurate Closed-Loop Temperature Control for Microfluidics Paper-Based Analytical Devices. *Microsyst. Technol.* **2018**, *24* (9), 3915−3924.
(26) Baldé, C. P.; Kuehr, R.; Yamamoto, T.; McDonald, R.; D'Angelo, H.; Althaf, S.; Bel, G.; Deubzer, O.; Fernandez-Cubillo, E.; Forti, V.; Gray, V.; Herat, S.; Honda, S.; Iatonni, G.; Khetriwal, D. S.; di Cortemiglia, V. L.; Lobuntsova, Y.; Nnorom, I.; Pralat, N.; Wagner, M. *Global E-Waste Monitor 2024*; International Telecommunication Union (ITU) and United Nations Institute for Training and Research (UNITAR): Geneva, Switzerland/Bonn, Germany, 2024; https://ewastemonitor.info/the-global-e-waste-monitor-2024/.
(27) Traiwattanapong, W.; Molahalli, V.; Pattanaporkratana, A.; Chattham, N. Recent Developments in Thermally Stable Transparent Thin Films for Heater Applications: A Systematic Review. *Nanomaterials* **2024**, *14* (24), 2011.
(28) Nguyen, V. H.; Papanastasiou, D. T.; Resende, J.; Bardet, L.; Sannicolo, T.; Jiménez, C.; Muñoz-Rojas, D.; Nguyen, N. D.; Bellet, D. Advances in Flexible Metallic Transparent Electrodes. *Small* **2022**, *18* (19), 2106006.
(29) Qin, Y.; Ouyang, X.; Lv, Y.; Liu, W.; Liu, Q.; Wang, S. A Review of Carbon-Based Conductive Inks and Their Printing Technologies for Integrated Circuits. *Coatings* **2023**, *13* (10), 1769.
(30) Papanastasiou, D. T.; Carlos, E.; Muñoz-Rojas, D.; Jiménez, C.; Pimentel, A.; Fortunato, E.; Martins, R.; Bellet, D. Fully Solution-Based AgNW/AlO $_x$ Nanocomposites for Stable Transparent Heaters. *ACS Appl. Electron. Mater.* **2022**, *4* (12), 5816−5824.
(31) Liu, Y.; Zhang, J.; Gao, H.; Wang, Y.; Liu, Q.; Huang, S.; Guo, C. F.; Ren, Z. Capillary-Force-Induced Cold Welding in Silver-Nanowire-Based Flexible Transparent Electrodes. *Nano Lett.* **2017**, *17* (2), 1090−1096.
(32) Zhang, K.; Li, J.; Fang, Y.; Luo, B.; Zhang, Y.; Li, Y.; Zhou, J.; Hu, B. Unraveling the Solvent Induced Welding of Silver Nanowires for High Performance Flexible Transparent Electrodes. *Nanoscale* **2018**, *10* (27), 12981−12990.

https://doi.org/10.1021/acsaelm.5c00305
ACS Appl. Electron. Mater. 2025, 7, 4862−4871